Materials Research Express

RECEIVED
23 December 2018

REVISED
28 February 2019

ACCEPTED FOR PUBLICATION
15 March 2019

PUBLISHED
29 March 2019

PAPER

Morphology and performance of pvdf membranes composed of triethylphospate and dimethyl sulfoxide solvents

Nasrul Arahman[1,2], **Sri Mulyati**[1] **and Afrillia Fahrina**[3]

[1] Department of Chemical Engineering, Universitas Syiah Kuala, Banda Aceh, Indonesia
[2] Graduate School of Environmental Management, Universitas Syiah Kuala, Banda Aceh, Indonesia
[3] Graduate School of Chemical Engineering, Universitas Syiah Kuala, Banda Aceh, Indonesia

E-mail: nasrular@unsyiah.ac.id

Keywords: polyvinylidene fluoride (PVDF), triethyl phosphate (TEP), dimethyl sulfoxide (DMSO), hansen solubility parameter

Abstract

This study investigated the impact of different solvents on the characteristics and filtration performance of polyvinylidene fluoride (PVDF) membranes. PVDF membranes were fabricated via the non-solvent induced phase separation (NIPS) technique by dissolving 20% w/w PVDF in triethyl phosphate (TEP) and dimethyl sulfoxide (DMSO), separately. The Hansen solubility parameter was studied as the kinetic aspect that influences membrane formation. The characteristics of the membranes were investigated including the membrane morphological structure, surface roughness, chemical group composition, and tensile strength. The filtration performance of the resulting membranes was also conducted using cross-flow filtration including pure water permeability (PWP), synthetic $CaCO_3$ suspension rejection, and membrane recovery after long-term filtration. The experimental results showed that DMSO has a closer solvent affinity with the non-solvent resulting in a membrane with higher porosity than the TEP membrane with a denser structure. Furthermore, the PVDF/DMSO membrane also had higher PWP than the PVDF/TEP membrane. However, in terms of the filtration performance of the $CaCO_3$ suspension, the PVDF/TEP membrane showed the best performance with higher flux permeation, better flux recovery of up to 96.6%, and the highest solute rejection reaching 100%. The analysis of the experimental results are discussed further.

1. Introduction

Base material selection in membrane manufacturing process is considerable importance to obtain membrane with outstanding performance. Almost all membranes are manufactured by means of the phase inversion method, especially the non-solvent induced phase separation (NIPS) technique due to its simplicity and flexibility [1]. Three main materials are needed in the NIPS technique: polymer, solvent, and non-solvent [2, 3]. The main materials influence and affect the membrane structure, characteristics, and performance during the filtration process [4].

Among the commercial polymers, polyvinylidene fluoride (PVDF) offers many advantages in the resulting membrane properties, such as good chemical resistance, excellent mechanical strength, and good thermal stability [1, 5]. The resulted membrane has been succesfully applied for water purification [6], domestic wastewater treatment [3], gas selection [7], and protein separation [8, 9]. The study was focused on the membrane material modification in relation to the structure formation. However, solvent selection as base material should be considered, especially for non-solvent induced phase separation (NIPS) method. The majority of the previous studies fabricated PVDF membranes using an organic non-solvent, such as dimethylformamide (DMF), dimethylacetamide (DMAc) or N-Methyl-2-pyrrolidone (NMP) [10, 11]. Hence, the resulting film has different types of structure and porosity.

In NIPS technique, the phase inversion or solidification process is complex, especially for semi-crystalline polymers, which may lead to liquid–liquid (L–L) demixing and solid–liquid (S–L) demixing simultaneously [12]. This is because the interaction between the solvent and the non-solvent is influenced by kinetic factors,

© 2019 IOP Publishing Ltd

such as mutual diffusivity or mutual [1, 13, 14]. In this case, the interaction of the polymers, solvent, and non-solvent are studied using the solubility parameter. Good affinity between the solvent and the polymer produces a membrane with uniform polymer configuration but might suffer from a low diffusion rate between the solvent and the non-solvent. Previous studies have confirmed that a poor diffusion rate between the solvent and the non-solvent results in a membrane that is less porous. In contrast, the high solidification process in a coagulation bath produces a membrane with high porosity and the formation of various macrovoids [14–16].

The filtration performance of membranes, including the permeability and selectivity, is mostly affected by the properties of the membrane, especially the morphological structure. A good membrane provides high permeability and good selectivity, as well as superior characteristics in terms of its hydrophilicity, mechanical properties, and thermal and chemical resistance. Therefore, in this study, different solvent for PVDF membrane fabrication was investigate to determine the characteristics and performance of resulting membranes. Solvent selection for this investigation are triethyl phosphate (TEP) and dimethylsulfoxide (DMSO)—which possesses different physicochemical properties. The characteristic of the membrane morphology, structure, surface roughness, tensile strength, and chemical compound are discussed.

2. Material and methods

2.1. Material

As the main polymer for membrane fabrication, Polyvinylidene fluoride (PVDF) with a molecular weight of 534,000 kDa was acquired from Sigma Aldrich, while triethylphospate (TEP) and dimethyl sulfoxide (DMSO), as solvents, with an analytical purity of 99% were purchased from Merck KGAa, Germany. Distilled water was used as a non-solvent. $CaCO_3$ with a molecular weight of 100,087 g mol^{-1} was applied as a synthesis foulant for the filtration test.

2.1.1. Membrane preparation

In this work, two series of membranes were prepared from the two polymer solutions. The first series of dope solutions was prepared by dissolving the PVDF in TEP; the fabricated membrane was labeled PVDF1. The second series of dope solutions were set by dissolving the PVDF in DMSO, and the resulting membrane was labeled PVDF2. The concentration of PVDF in both solutions was set constant at 20 wt%. The homogenous dope solution was achieved by agitating the solution using a magnetic stirrer for about 24 h., followed by leaving the solution at room temperature until the air bubbles released completely. A 200 μm thickness membrane applicator produced by Yoshimitsu, Japan (YBA-4) was used to form the membrane. Deionized water was used as the coagulation media of the membrane for all the experiments. The fabricated membranes were kept in distilled water overnight to remove any remaining solvent.

2.2. Characterization

2.2.1. Membrane preparation

Scanning electron microscopy (SEM, JSM-7500F, JEOL Ltd, Japan), and atomic force microscopy (AFM; SII NanoTechnology, Inc., Tokyo, Japan, SPA400) were employed to analyze the morphology of the membranes. SEM was used to investigate the structure of the pore formation on the top surface and the cross-section of the membrane, while AFM was used to determine the roughness of the membrane surface by counting the average nodule size. For the SEM and AFM measurement, the membrane samples were immersed in liquid nitrogen for about two minutes, followed by freeze drying overnight at a temperature of −55 °C and vacuum pressure of 16.6 Pa. For the AFM analysis, the dried membrane was placed directly in the AFM chamber, while an osmium coating was provided for SEM measurement.

2.2.2. Chemical composition

Scanning electron microscopy (SEM, JSM-7500F, JEOL Ltd, Japan), and atomic force microscopy (AFM; SII NanoTechnology, Inc., Tokyo, Japan, SPA400) were employed to analyze the morphology of the membranes. SEM was used to investigate the structure of the pore formation on the top surface and the cross-section of the membrane, while AFM was used to determine the roughness of the membrane surface by counting the average nodule size. For the SEM and AFM measurement, the membrane samples were immersed in liquid nitrogen for about two minutes, followed by freeze drying overnight at a temperature of −55 °C and vacuum pressure of 16.6 Pa. For the AFM analysis, the dried membrane was placed directly in the AFM chamber, while an osmium coating was provided for SEM measurement.

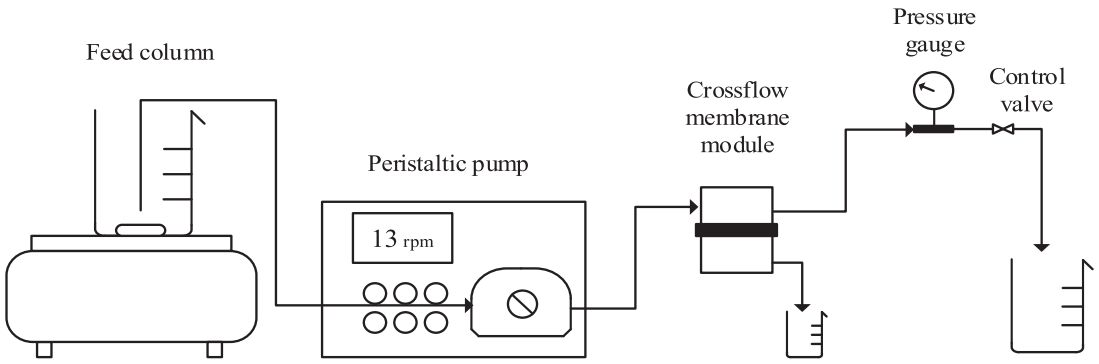

Figure 1. Crossflow filtration system.

2.2.3. Mechanical properties

The mechanical properties of the membranes were observed in terms of membrane strength and elongation at break. The properties were analyszed using a tensile strength test instrument (Autograph AGS-J, Shimadzu Co. Japan). The membrane samples were prepared with dimensions in accordance with the AGS-J System Standard. For investigation of the mechanical properties, the measurements were taken three times for each sample to ensure accurate data.

2.3. Filtration

2.3.1. Water purification

The water purification test was designed using a single piece membrane with an effective area of 9,075 cm^2 by means of the crossflow-filtration module. A turbid water sample was prepared by dissolving 2 g $CaCO_3$ in 1 L of distilled water. The filtration was conducted at room temperature and a constant trans-membrane pressure (TMP) of 2 bars. The water was forced through the membrane using a peristaltic pump (Watson Marlow Sci-323) with a rotation speed of 13 rpm and the filtration was conducted for 300 min. The experimental set up for the crossflow filtration system is shown in figure 1. The water flux of the membrane and the amount of turbidity parameter removed from the water sample was calculated using equations (1) and (2), respectively.

$$Water\ Flux\left(\frac{L}{m^2.h}\right)=\left(\frac{V}{A.t}\right) \tag{1}$$

$$Rejection\ (\%)=\left(1-\frac{C_p}{C_f}\right) \tag{2}$$

In which,

V = volume of permeated water (L)
A = is the effective membrane area (m^2)
t = permeation time (h)
P = trans-membrane pressure (bar)
C_f = $CaCO_3$ concentration in feed
C_p = $CaCO_3$ concentration in permeate

3. Results

3.1. Membrane morphology

The use of different solvents in membrane manufacturing could result in the formation of different structures [17]. In this inversion phase technique, the interaction of the solvent and non-solvent during membrane solidification has a significant impact on the membrane structure and morphology [16]. The solvent (S) affinity towards the non-solvent (NS) affects the exchange rate of the solvent in the coagulation bath and the non-solvent in the polymer solutions. A closer affinity accelerates the exchange rate of S-NS resulting in a more porous membrane [17, 18]. As can be seen in figure 2, the SEM images of the PVDF1 and PVDF2 membranes show different structures.

The PVDF1 membrane made of PVDF/TEP shows a denser structure on the top surface with a less porous support layer than that of PVDF2, which was made using the PVDF/DMSO system. The large macrovoid finger like structure in the PVDF/DMSO system is clearly seen in figure 2. The fast phase inversion rate led to higher

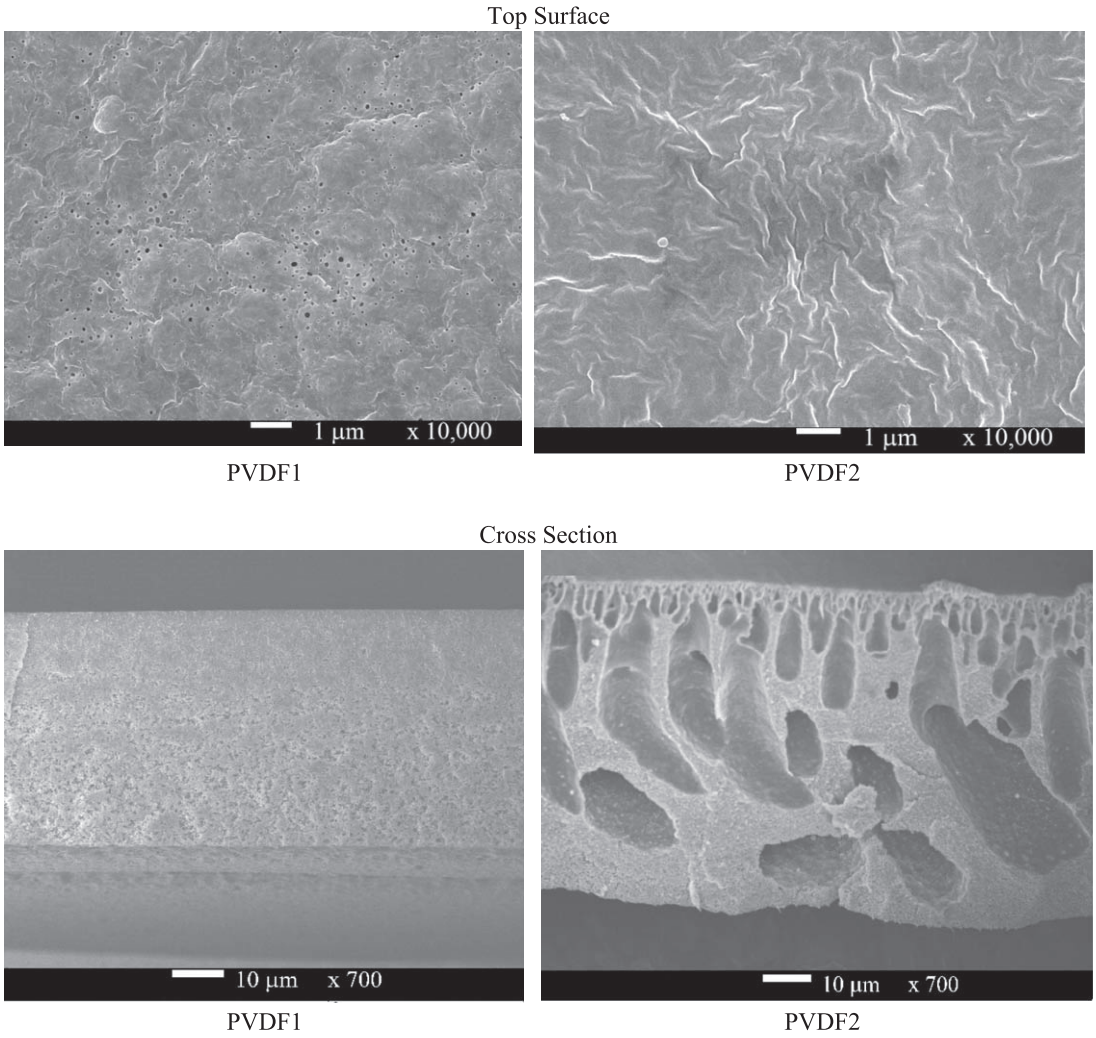

Figure 2. SEM image of membrane surface and cross-section.

Table 1. Hansen solubility parameter data of materials used.

Materials	Solubility parameters, δ (Mpa)$^{1/2}$
PVDF	23, 2
TEP	22, 3
DMSO	26, 7
Water	47, 8

pore formation compared to the lower exchange rate of the S-NS, which cause delayed demixing and the forming of narrow membrane structures [18, 19]. The influence of the S-NS interaction on the rate of solidification process can be studied using the 'solubility parameter' of the solvent and polymer [20], which can be calculated using the Hansen equation (equation (3)).

$$\delta = \sqrt{\delta_d^2 + \delta_p^2 + \delta_h^2} \tag{3}$$

δ_d, δ_p, δ_h is the notation of the interaction of dispersion (d), polar bond (p), and hydrogen bond (h), respectively. The solubility parameters of the PVDF, solvents, and non-solvent used in this study are depicted in table 1.

According to table 1, the solubility parameter of TEP is closer to that of PVDF than for DMSO, but inversely correlated to water. In other words, TEP dissolves more easily in PVDF than in DMSO, which results in the uniform surface of the membrane, as can be seen in figure 2. In comparing the PVDF2 membrane with the PVDF/DMSO system, aggregation of the polymer is visible on the top surface due to the weak solvent [1]. However, the pore formation on the support layer is strongly correlated to the interaction between the solvent and the non- solvent, which is indicated by the solubility parameter. Table 1 shows that DMSO has a closer

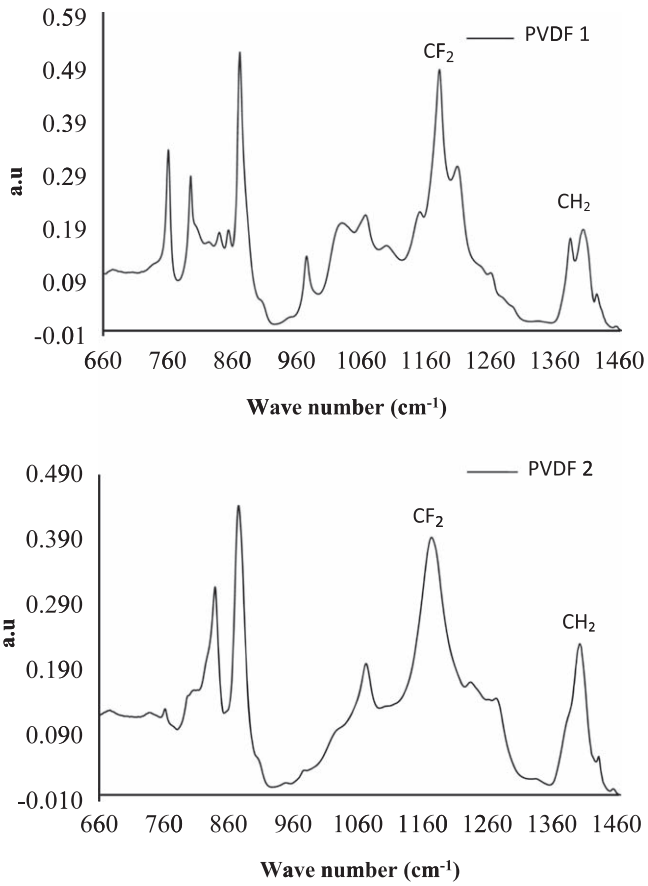

Figure 3. FTIR spectra of the PVDF1 and PVDF2 membranes.

affinity with water than the TEP solvent. When the casting solution was immersed in the sequencing bath, DMSO immediately leached out from the polymer solution and was substituted with water from the bath. The fast exchange rate of DMSO and water triggered the formation of macrovoids on the membrane structure [16]. In contrast to the PVDF/TEP system, the distant solubility parameter of the solvent towards the water leads to a slow solidification process and, ultimately, a membrane with a symmetric structure and almost no cavities; as shown in figure 1. The same result has been previously reported by other researchers [13, 21].

3.2. The composition of the fabricated membrane

Figure 3 shows the FTIR spectra of the PVDF membrane with different solvents. For both membranes, the out-of-plane C–H bending vibrations appeared in the region of 650–900 cm^{-1} At 972 cm^{-1}, the alkene group in the PVDF1 membrane is indicated by the C–H bending. The alcohol group (C–O) is observed at peak 1082 cm^{-1} and 1068 cm^{-1} for the PVDF1 membrane and the PVDF2 membrane, respectively. The strong peak at 1179 cm^{-1} in the PVDF1 membrane and the strong peak absorbed at 1168 cm^{-1} in the PVDF2 membrane indicates the CF_2 bond. Asymmetric CH_2 shows at peak 1400 cm^{-1} in PVDF1 and at 1398 cm^{-1} in PVDF2 membrane. The presence of CF_2 and CH_2 in the spectra of both membranes shows the characteristics of PVDF as a membrane material [22]. The chemical structure of the PVDF polymer is shown in figure 4.

3.3. Surface roughness

The properties of the membrane surface were investigated using atomic force microscopy (AFM), which confirmed the roughness of the membrane surface at the nano-scale. The 3D AFM images of the top surface of the PVDF membrane for both systems investigated in this work are shown in figure 5. In all cases, the membrane has a nodular structure that consists of peaks with a bright area and valleys with a dark area. The averages of the differences between the highest peaks and the lowest valleys are counted as the membrane surface roughness (Ra). The PVDF1 membrane has a roughness of 10.82 nm, whereas PVDF2 has a surface roughness of 11.39 nm. These results indicate that the surface of the PVDF2 membrane has greater roughness than that for PVDF1. The surface roughness of the membrane could lead to fouling or particles in the solution clogging the pores of the membrane easier and, thus, forming a cake layer [23]. In the filtration process, membranes with a rougher surface have a tendency for fouling and a decline in the flux permeation [24].

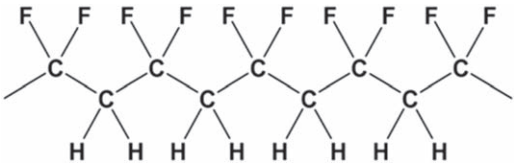

Figure 4. Polymer structure of polyvinylidene fluoride.

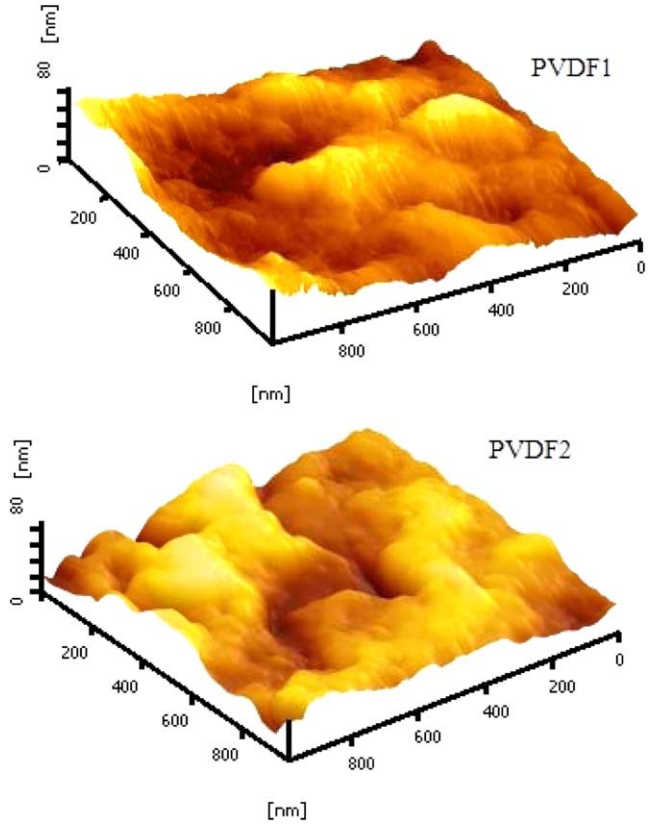

Figure 5. AFM image of PVDF1 and PVDF2 membrane.

Some researchers have investigated the effect of the surface roughness of the membranes on the filtration flux and fouling phenomena on the membrane [25, 26]. The research group of Min compared the surface roughness of two PVDF membranes with the same chemical-physics characteristics on the filtration flux. Filtration was carried out to filter the solution of humic acid and calcium acid [27]. The results showed that membranes with rough surfaces had lower flux due to higher fouling than that for smooth membranes.

3.4. Mechanical properties

The investigation of the mechanical properties of the membranes was conducted using the tensile strength test. Excellent mechanical properties mean that the membranes have high durability and the ability to cope with high pressure. As shown in figure 6, the tensile strengths of both membranes are significantly different. The PVDF1 membrane provides high tensile strength of about 16.188 Mpa, while the tensile strength of the PVDF2 membrane is only around 2.479 Mpa. For this reason, the porosity of the membrane clearly affects the tensile strength of the membrane. The large macrovoids in the structure of the PVDF2 membrane weaken the membrane meaning that it would be easily damaged by further pressure [18, 28]. In contrast, the PVDF1 membrane with almost no cavities and less porosity displays good tensile strength due to the strong polymer matrix and dense structure.

3.5. Filtration performance

The filtration performance of the PVDF membrane on the water purification process is presented in figure 7 and figure 8. Based on figure 7, the filtration flux of the resulting membrane tends to decrease over time.

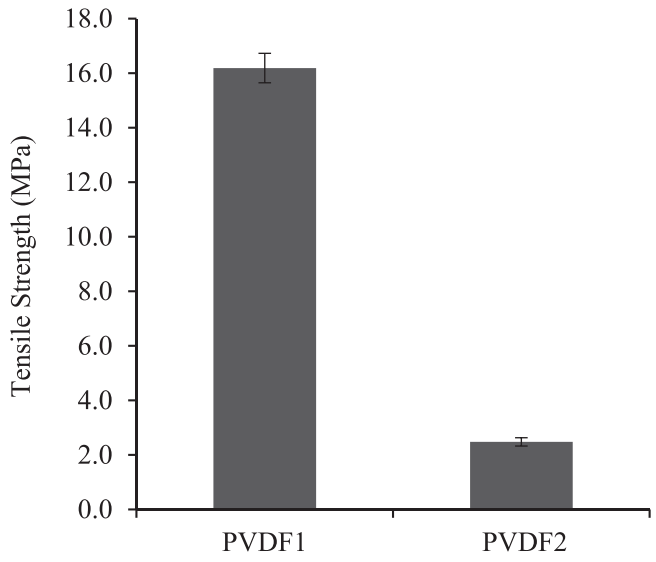

Figure 6. Mechanical properties of PVDF1 and PVDF2 membranes.

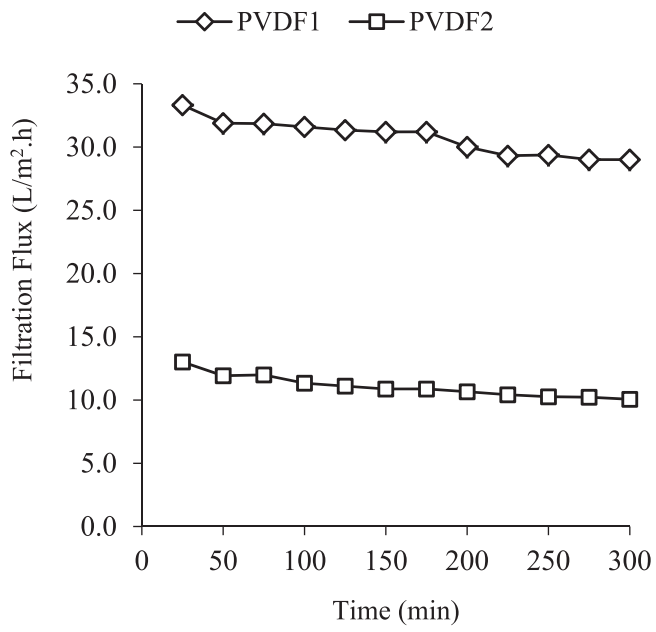

Figure 7. Filtration flux of $CaCO_3$ solution.

Furthermore, as observed in figure 7, the PVDF1 membrane has higher flux than the PVDF2 membrane. According to the AFM investigation in figure 4, the PVDF2 membrane has a rougher surface than the PVDF1 membrane and, thus, exhibits fouling phenomena. The rougher surface, which consists of valleys, causes fouling or blockage of the membrane pores by the $CaCO_3$ particles contained in the water sample.

During the filtration process, the $CaCO_3$ particles that clog the membrane pores increase and form a cake layer on the upper layer of the membrane. Such a condition greatly inhibits the permeate rate of the membrane, and, thus, results in declining of the permeate flux [29, 30]. The same result for humid acid solution filtration was reported by Woo and co worker that smooth membrane surface provide higher flux that the rough membrane [29]. However, the rejection results of both the fabricated membranes are shown to be satisfactory; as can be seen in figure 8.

All of the membranes provided a high rejection of above 99.5%, with the PVDF1 membrane retaining 100% of the $CaCO_3$ particles. Based on the SEM image of the PVDF1 membrane in figure 2, the PVDF1 membrane has a dense structure, while the PVDF2 membrane has large macrovoids. In terms of the filtration performance, the dense structure of the PVDF1 membrane provides superior rejection of the particles to that of the PVDF2

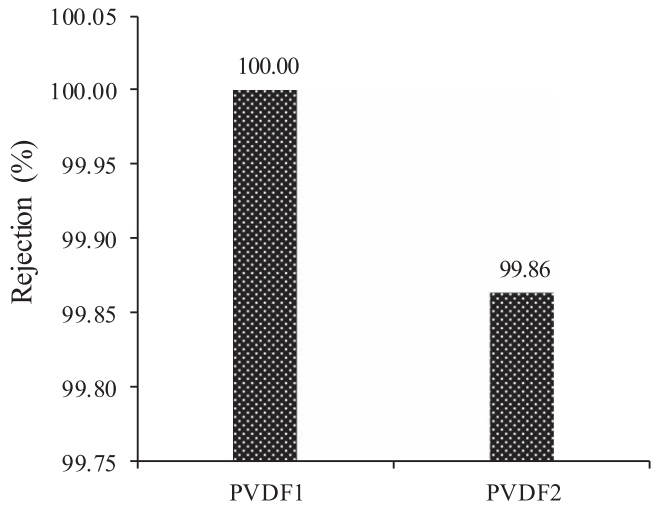

Figure 8. Solute rejection of performance.

Figure 9. Comparison of the sample solutions before and after filtration by the PVDF1 membrane.

Table 2. The performance of PVDF membrane prepared by various non solvent.

PVDF (%)	Solvent	Non-solvent	Filtration Flux (L/m^2.h)	Rejection (%)/sample	Tensile (Mpa)	References
20	TEP	Water	29 ± 0.3	100/ $CaCO_3$	18.21	This work
20	DMSO	Water	10 ± 0.)	99.86/$CaCO_3$	2.48	This work
20	NMP	Water	14.2	87.3/BSA	—	[31]
19	DMAc	Ethanol-water	30	95.9/α-amylase	13.2031	[32]
17.5	DMF	0.3%				
SLS-water	4.8 ± 0.3	98, 4)/ RB5 dye	—	[33]		

membrane [29]. The porous of membrane could lead to the $CaCO_3$ particles passing through the membrane pores due to trans-membrane pressure. In addition, the accumulation of particles in the membrane pores of the PVDF2 membrane will result in more particles permeating the membrane and lower filtration quality. A comparison of the $CaCO_3$ solution before and after filtration using the best membrane rejection (PVDF1) is shown in figure 9. Some researchers have reported the study of PVDF membrane preparation by using others solvent. The comparison of the membrane performances resulted in this work and other study is listed in table 2.

4. Conclusion

In this study, the fabrication, characterization, and the performance of the PVDF membranes using two different solvents has been reported. The kinetic factors as the solubility parameter, δ, of the materials impacted on the membrane structures. The membrane surface was affected by the closeness of the solubility parameter between the polymer and the solvent, while the support layer of the membranes was influenced by the closeness of the solubility parameter between the solvent and the non-solvent. The use of TEP as the solvent resulted in a PVDF membrane with a uniform and dense structure, while the application of DMSO in the membrane composition led to the formation of pores and a fingerlike structure with large macrovoids in the membrane support layer. The PVDF/TEP membrane with its dense structure is superior in terms of surface roughness, mechanical properties, and filtration performance. According to the tensile test, the PVDF/TEP membrane has a tensile strength of up to 18.21 MPa, while the tensile strength of the PVDF/DMSO membrane is only 2.48 Mpa. The influence of the surface roughness of the membrane also affects the membrane filtration. The PVDF/TEP with a smoother surface, Ra = 10.82 nm, compared to the PVDF/DMSO, Ra = 11.39, experienced lower fouling phenomena, and, thus, showed higher flux during $CaCO_3$ filtration. However, both membranes showed satisfactory performance—the PVDF/TEP membrane could retain 100% of the $CaCO_3$ particles, compared to 99.8% for the PVDF/DMSO membrane.

Acknowledgments

Appreciation to the University of Syiah Kuala, Banda Aceh Indonesia for funding support of this research via PCP Research Grant.

ORCID iDs

Nasrul Arahman https://orcid.org/0000-0001-5077-2867

References

[1] Liu F, Hashim N A, Liu Y, Abed M R M and Li K 2011 Progress in the production and modification of PVDF membranes *J. Memb. Sci.* **375** 1–27
[2] Ulbricht M 2006 Advanced functional polymer membranes *Polymer (Guildf)* **47** 2217–62
[3] Mavukkandy M O, Bilad M R, Kujawa J, Al-Gharabli S and Arafat H A 2017 On the effect of fumed silica particles on the structure, properties and application of PVDF membranes *Sep. Purif. Technol.* **187** 365–73
[4] Pezeshk N, Rana D, Narbaitz R M and Matsuura T 2012 Novel modified PVDF ultrafiltration flat-sheet membranes *J. Memb. Sci.* **389** 280–6
[5] Muchtar S, Wahab M Y, Fang L, Jeon S, Rajabzadeh S, Takagi R, Mulyati S, Arahman N and Riza M 2018 Polydopamine-coated poly (vinylidene fl uoride) membranes with high ultraviolet resistance and antifouling properties for a photocatalytic membrane reactor *J. Appl. Sci.* **47312** 1–9
[6] Wang T, Wang Z, Wang P and Tang Y 2019 An integration of photo-fenton and membrane process for water treatment by a PVDF @ $CuFe_2O_4$ catalytic membrane *J. Memb. Sci.* **572** 419–27
[7] Rajati H, Navarchian A H and Tangestaninejad S 2018 Preparation and characterization of mixed matrix membranes based on matrimid/PVDF blend and MIL-101 (Cr) as filler for CO_2/CH_4 separation *Chem. Eng. Sci.* **185** 92–104
[8] Saraswathi M S S A, Rana D, Divya K, Alwarappan S and Nagendran A 2018 Fabrication of anti-fouling PVDF nanocomposite membranes using manganese dioxide nanospheres with tailored morphology, hydrophilicity and permeation *New J. Chem.* **42** 15803
[9] Abirami M S, Kausalya R, Jacob N, Rana D and Nagendran A 2017 Journal of environmental chemical engineering BSA and humic acid separation from aqueous stream using polydopamine coated PVDF ultra fi ltration membranes *J. Environ. Chem. Eng.* **5** 2937–43
[10] Tomaszewska M 1996 Preparation and properties of flat-sheet membranes from poly (vinylidene fluoride) for membrane distillation *Desalination* **104** 1–11
[11] Sun C and Feng X 2017 Enhancing the performance of PVDF membranes by hydrophilic surface modification via amine treatment *Sep. Purif. Technol.* **185** 94–102
[12] Zheng L, Wu Z, Zhang Y, Wei Y and Wang J 2016 Effect of non-solvent additives on the morphology , pore structure , and direct contact membrane distillation performance of PVDF-CTFE hydrophobic membranes *J. Environ. Sci.* **45** 28–39
[13] Bottino A, Camera-Roda G, Capannelli G and Munari S 1991 The formation of microporous polyvinylidene difluoride membranes by phase separation *J. Memb. Sci.* **57** 1–20
[14] Wang Q, Wang Z and Wu Z 2012 Effects of solvent compositions on physicochemical properties and anti-fouling ability of PVDF micro fi ltration membranes for wastewater treatment *DES* **297** 79–86
[15] Arahman N, Maruyama T, Sotani T and Matsuyama H 2008 Effect of hypochlorite treatment on performance of hollow fiber membrane prepared from polyethersulfone/N-methyl-2-pyrrolidone/tetronic 1307 solution *J. Appl. Polym. Sci.* **110** 687–94
[16] Nikooe N and Saljoughi E 2017 Preparation and characterization of novel PVDF nanofiltration membranes with hydrophilic property for filtration of dye aqueous solution *Appl. Surf. Sci.* **413** 41–9
[17] Yeow M L, Liu Y T and Li K 2004 Morphological study of poly (vinylidene fluoride) asymmetric membranes: effects of the solvent, additive, and dope temperature *J. Appl. Polym. Sci.* **92** 1782–9
[18] Shen J, Ruan H, Wu L and Gao C 2011 Preparation and characterization of PES—SiO_2 organic—inorganic composite ultrafiltration membrane for raw water pretreatment **168** 1272–8

[19] Marques F, Rezzadori K, Carolina M, Zanatta V, Zin G, Walker D, De Oliveira J V, Carlos J, Petrus C and Di M 2015 Influence of different solvent and time of pre-treatment on commercial polymeric ultrafiltration membranes applied to non-aqueous solvent permeation *Eur. Polym. J.* **66** 492–501
[20] Penha F M, Rezzadori K, Proner M C, Zanatta V, Zin G, Tondo D W, De Oliveira J V, Petrus J C C and Di Luccio M 2015 Influence of different solvent and time of pre-treatment on commercial polymeric ultrafiltration membranes applied to non-aqueous solvent permeation *Eur. Polym. J.* **66** 492–501
[21] Yeow M L, Liu Y T and Li K 2004 Morphological study of poly(vinylidene fluoride) asymmetric membranes: effects of the solvent, additive, and dope temperature *J. Appl. Polym. Sci.* **92** 1782–9
[22] Yuliwati E, Ismail A F, Matsuura T, Kassim M A and Abdullah M S 2011 Effect of modified pvdf hollow fiber submerged ultrafiltration membrane for refinery wastewater treatment *Desalination* **283** 214–20
[23] Goodyer C E and Bunge A L 2012 Mass transfer through membranes with surface roughness *J. Memb. Sci.* **409–410** 127–36
[24] Abdel-karim A, Gad-allah T A, El-kalliny A S, Ahmed S I A, Souaya E R, Badawy M I and Ulbricht M 2017 Fabrication of modified polyethersulfone membranes for wastewater treatment by submerged membrane bioreactor *Sep. Purif. Technol.* **175** 36–46
[25] Hobbs C, Hong S and Taylor J 2006 Effect of surface roughness on fouling of RO and NF membranes during filtration of a high organic surficial groundwater *J. Water. Supply. Res. T.* 559–70
[26] Zhong Z, Li D, Zhang B and Xing W 2012 Membrane surface roughness characterization and its influence on ultrafine particle adhesion *Sep. Purif. Technol.* **90** 140–6
[27] Woo S H, Park J and Min B R 2015 Relationship between permeate flux and surface roughness of membranes with similar water contact angle values *Sep. Purif. Technol.* **146** 187–91
[28] Lv C, Su Y, Wang Y, Ma X, Sun Q and Jiang Z 2007 Enhanced permeation performance of cellulose acetate ultrafiltration membrane by incorporation of Pluronic F127 *J. Memb. Sci.* **294** 68–74
[29] Woo S H, Lee J S and Min B R 2017 Change of surface morphology, permeate flux, surface roughness and water contact angle for membranes with similar physicochemical characteristics (except surface roughness) during Microfiltration *Sep. Purif. Technol.* **187** 274–84
[30] Sheng A L K, Bilad M R, Osman N B and Arahman N 2017 Sequencing batch membrane photobioreactor for real secondary effluent polishing using native microalgae: process performance and full-scale projection *J. Clean. Prod.* **168** 708-15
[31] Shen J, Zhang Q, Yin Q, Cui Z, Li W and Xing W 2017 Fabrication and characterization of amphiphilic PVDF copolymer ultra fi ltration membrane with high anti-fouling property *J. Memb. Sci.* **521** 95–103
[32] Yan L, Shui Y, Bao C and Xianda S 2006 Effect of nano-sized Al_2O_3-particle addition on PVDF ultrafiltration membrane performance *J. Memb. Sci.* **276** 162–7
[33] Srivastava H P, Arthanareeswaran G, Anantharaman M and Starov V M 2011 Performance of modi fi ed poly (vinylidene fl uoride) membrane for textile wastewater ultra fi ltration *Desalination* **282** 87–94